

Supplemental information

**Defects in NK cell immunity of pediatric
cancer patients revealed by deep immune profiling**

Eleni Syrimi, Naeem Khan, Paul Murray, Carrie Willcox, Tracey Haigh, Benjamin Willcox, Navta Masand, Claire Bowen, Danai B. Dimakou, Jianmin Zuo, Sierra M. Barone, Jonathan M. Irish, Pamela Kearns, and Graham S. Taylor

Supplementary Figures and Tables

Table S1

Paediatric Healthy			Paediatric Cancer			
Study Number	Age	Gender	Study Number	Age	Gender	Disease
HV01	37m	Female	C01	79m	Female	Rhabdomyosarcoma
HV05	12m	Male	C02	73m	Male	Burkitt's lymphoma
HV06	17m	Female	C03	36m	Female	Neuroblastoma
HV11	19m	Male	C04	167m	Female	Hodgkin's disease
HV12	72m	Female	C05	58m	Male	Wilms
HV13	170m	Female	C06	187m	Female	Rhabdomyosarcoma
HV14	20m	Female	C07	122m	Male	Hodgkin's disease
HV15	22m	Male	C08	20m	Male	Neuroblastoma
HV16	78m	Male	C09	17m	Female	Rhabdoid tumour
HV18	15m	Male	C10	145m	Female	Burkitt's lymphoma
HV20	110m	Female	C11	17m	Male	Neuroblastoma
HV21	74m	Female	C12	22m	Female	Pilomyxoid astrocytoma
HV22	42m	Male	C14	179m	Female	Ewing's sarcoma
HV25	77m	Male	C15	187m	Male	Hodgkin's disease (non classical NHPHL)
HV26	12m	Female	C16	12m	Male	Neuroblastoma
HV28	35m	Male	C18	36m	Female	Hepatoblastoma
HV30	126m	Male	C19	12m	Male	Nephroblastomatosis
HV34	174m	Female	C20	73m	Male	Hodgkin's disease
HV37	54m	Female	C21	34m	Male	Burkitts lymphoma
			C22	75m	Female	Parameningeal Rhabdomyosarcoma

Table S1. Demographic data for the paediatric healthy donors and paediatric cancer patients (discovery cohort), related to Figures 1 and 2. The diagnosis for each patient is also shown. Age is provided in months.

Table S2

Metal	Marker	Clone	Source
89Y	CD45 (BC)	H130	Fluidigm
114 Qdot	CD45 (BC)	H130	Biolegend
115In	CD45 (BC)	H130	Biolegend
141Pr	CD31	WM59	Biolegend
142Nd	CD57	HCD57	Fluidigm
143Nd	CD38	HIT2	Biolegend
144Nd	CD8	SK1	Biolegend
145Nd	CD4	RPA-T4	Fluidigm
146Nd	IgD	IA6-2	Fluidigm
147Sm	CXCR3	G025H7	Biolegend
148Sm	CD16	3G8	Fluidigm
149Sm	CD127	AO19D5	Fluidigm
150Nd	OX40	ACT35	Fluidigm
151Eu	CCR6	G034E3	Biolegend
152Sm	TCR-gd	11F2	Fluidigm
153Eu	CCR4	L291H4	Biolegend
154Sm	CD73	AD2	Biolegend
155Gd	PD1	EH12.2H7	Fluidigm
156Gd	CD45RA	HI100	Biolegend
158Eu	CD33	WM53	Fluidigm
159Tb	CD161	HP-3G10	Fluidigm
160Gd	CD39	A1	Fluidigm
161Dy	ICOS	C398.4A	Biolegend
162Dy	CD27	L128	Fluidigm
163Dy	CD56	NCAM16.2	Fluidigm
164Dy	CD95	DX2	Fluidigm
165Ho	CD19	HB19	Fluidigm
166Er	CD24	ML5	Fluidigm
167Er	CCR7	G043H7	Biolegend
168Er	CXCR5	J252D4	Biolegend
169Tm	CD25	2A3	Fluidigm
170Er	CD123	6H6	Biolegend
171Yb	CD5	UCHT2	Biolegend
172Yb	CD11c	3.9.	Biolegend
173Yb	CD3	UCHT1	Biolegend
174Yb	HLA-DR	L243	Fluidigm
175Lu	CD14	M5E2	Fluidigm
176Yb	TCR va7.2	3C10	Biolegend
194-198Pt	CD45 (BC)	H130	Biolegend
209Bi	CD11b	ICRF44	Fluidigm

Table S2. Mass cytometry antibody panel used to characterise the immune cell phenotype of the discovery cohort, related to Figures 1 and 2. CD45-specific antibodies used for barcoding are indicated with (BC) in the table.

Table S3

Metal	Marker	Clone	Source
89Y			
114 Qdot			
115In	CD45 (BC)	H130	Biolegend
141Pr	gamma-delta 2	123R3	Milteny
142Nd	CD57	HCD57	Fluidigm
143Nd			
144Nd	CD8	SK1	Biolegend
145Nd	CD4	RPA-T4	Fluidigm
146Nd			
147Sm	CXCR3	G025H7	Biolegend
148Sm	CD16	3G8	Fluidigm
149Sm	CD127	AO19D5	Fluidigm
150Nd			
151Eu	CCR6	G034E3	Biolegend
152Sm	CD27	M-T271	
153Eu	CX3CR1	2A91	Biolegend
154Sm	TIGIT	A15153G	Biolegend
155Gd	PD1	EH12.2H7	Fluidigm
156Gd	CD45RA	HI100	Biolegend
158Eu			
159Tb	Nkp30	Z25	Fluidigm
160Gd	gamma-delta 1	REA173	Milteny
161Dy			
162Dy	Nkp46	BAB281	Fluidigm
163Dy	CD56	NCAM16.2	
164Dy	CD95	DX2	
165Ho	1 ^o NKG2C-PE 2 ^o Anti-PE	134591, PE2	R&D Biosystems, Fluidigm
166Er	NKG2D	ON72	Fluidigm
167Er	CCR7	G043H7	Biolegend
168Er	CXCR5	J252D4	Biolegend
169Tm	NKG2A	Z199	Fluidigm
170Er	CD161	HP3610	Biolegend
171Yb	DNAM	DX11	Fluidigm
172Yb			
173Yb	CD3	UCHT1	Biolegend
174Yb			
175Lu	CD14	M5E2	Fluidigm
176Yb	TCR- α 7.2	3C10	Biolegend
194Pt	CD45 (BC)	H130	Biolegend
198Pt	CD45 (BC)	H130	Biolegend
209Bi	CD11b	ICRF44	Fluidigm

Table S3. Mass cytometry antibody panel used to characterise NK cell phenotype (discovery cohort), related to Figure 3. CD45-specific antibodies used for barcoding are indicated with (BC) in the table.

Table S4

Fluorochrome	Antibody	Clone	Source
e450	CD3	SK7	eBioscience
APC	CD56	CMSSB	eBioscience
PeCy7	CD16	eBioCB16	eBioscience
PerCP-Cy5.5	CD57	QA17A04	Biolegend
FITC	CD107a	H4A3	Biolegend
AF700	TNF-a	Mab11	Biolegend
PE	INF-g	4S.B3	Biolegend
APC-Cy7	CD19	HIB19	eBioscience
APC-Cy7	CD14	6ID3	eBioscience
APC-Cy7*	Live-Dead		Biolegend
PeCy7	perforin	dG9	eBioscience
PE-texas red	granzyme b	GB11	Invitrogen

Table S4. Fluorescent flow cytometry antibody panel used for further NK cell characterisation, related to Figure 3. *e-Fluor 780 live dead stain detected on APC-CY7 detector.

Table S5

Paediatric Healthy			Paediatric Cancer			
Study Number	Age	Gender	Study Number	Age	Gender	Disease
HV04	16m	Female	C23	56m	Female	Wilms
HV07	7m	Male	C24	172m	Female	Hodgkins Disease
HV11	19m	Male	C25	29m	Male	Neuroblastoma
HV12	72m	Female	C26	167m	Female	Osteosarcoma
HV13	170m	Female	C27	179m	Male	Hodgkins Disease
HV14	20m	Female	C28	59m	Male	Rhabdomyosarcoma
HV15	22m	Male	C29	51m	Male	Rhabdomyosarcoma
HV16	78m	Male	C30	189m	Female	Ewings sarcoma
HV19	51m	Male	C31	176m	Male	Hodgkins Disease
HV21	74m	Female	C32	118m	Male	Hodgkins Disease
HV23	30m	Male	C33	130m	Female	Ewings sarcoma
HV24	137m	Female	C34	47m	Female	Wilms
HV25	77m	Male	C35	183m	Male	Osteosarcoma
HV27	109m	Male	C36	19m	Female	Wilms
HV30	126m	Male	C37	38m	Female	Wilms
HV31	11m	Male	C38	32m	Male	Embryonal supratentorial tumour
HV37	54m	Female	C39	143m	Male	Osteosarcoma
HV38	153m	Male	C40	163m	Female	Hodgkins Disease
HV39	147m	Female	C41	162m	Male	Mixed Germ Cell Tumour
HV40	155m	Male	C42	149m	Male	Rhabdomyosarcoma
HV41	154m	Male	C44	87m	Male	B-cell Lymphoma
HV42	150m	Male	C45	189m	Male	Hodgkins Disease
HV43	155m	Male	C46	86m	Male	Rhabdomyosarcoma
HV44	124m	Male	C47	4m	Female	Rhabdoid tumour
			C48	170m	Male	Hodgkins disease
			C49	188m	Female	Rhabdoid tumour
			C50	88m	Female	Hepatoblastoma
			C51	65m	Male	Rhabdomyosarcoma
			C52	152m	Male	Rhabdomyosarcoma
			C53	158m	Female	Osteosarcoma
			C54	169m	Female	Ewings sarcoma

Table S5. Demographic data for the paediatric healthy donors and paediatric cancer patients (validation cohort), related to Figures 4 and 5. The diagnosis for each patient is also shown. Age is provided in months.

Table S6

Metal	Marker	Clone	Source	Metal	Marker	Clone	Source
89Y	CD45 (BC)	HI30	Fluidigm	161Dy	ILT3	ZM4.1	Biolegend
106Cd	CD45 (BC)	HI30	Biolegend	161Dy	ILT5	222821	R&D Systems
110Cd	CD45 (BC)	HI30	Biolegend	161Dy	ILT4	42D1	Fluidigm
111Cd	CD38	HIT2	Biolegend	162Dy	NKp44	P44-8	Biolegend
112Cd	CCR2	K036C2	Biolegend	162Dy	NKp46	BAB281	Fluidigm
114Cd	CD8a	SK1	Biolegend	163Dy	CXCR4	12G5	Biolegend
115In	CD57	HNK-1	Biolegend	163Dy	CXCR3	G025H7	Fluidigm
116Cd	CD36	5-271	Biolegend	164Dy	CD161	HP3G10	Fluidigm
141Pr	CD3	UCHT1	Fluidigm	165Ho	KIR2DS4	179315	R&D Systems
142Nd	CD19	HIB19	Fluidigm	166Er	NKG2D	ON72	Biolegend
143Nd	CD45RA	HI100	Fluidigm	167Er	KIR3DL1	DX9	Fluidigm
144Nd	CD69	FN50	Fluidigm	167Er	KIR3DL2	539304	R&D Systems
145Nd	CD4	RPA-T4	Fluidigm	168Er	CD127	A019D5	Fluidigm
146Nd	KIR2DL1/S1/S3/S5	HP-MA4	Biolegend	169Tm	NKG2A	Z199	Fluidigm
147Sm	CXCR1	42705	R&D Systems	170Er	CD122	Tu27	Fluidigm
147Sm	CXCR2	5E8/CXCR2	Fluidigm	171Yb	CD226	DX11	Fluidigm
148Nd	CD14	RMO52	Fluidigm	172Yb	CX3CR1	2A9-1	Fluidigm
149Sm	CD25	2A3	Fluidigm	173Yb	KIR2DL2/L3	DX27	Fluidigm
150Nd	CD27	LG.3A10	Fluidigm	173Yb	KIR2DL5	UP-R1	Miltenyi Biotec
151Eu	KIR2DL1/S5	143211	R&D Systems	174Yb	CD94	HP-3D9	Fluidigm
152Sm	ILT1	337902	Biolegend	175Lu	PD-1	EH12.2H7	Fluidigm
153Eu	CXCR5	RF8B2	Fluidigm	176Yb	KIR2DL4	181703	R&D Systems
154Sm	TIGIT	MBSA43	Fluidigm	194Pt	CD45 (BC)	HI30	Biolegend
154Sm	TIM3	F38-2E2	Fluidigm	195Pt	CD45 (BC)	HI30	Biolegend
155Gd	CD56	B159	Fluidigm	196Pt	CD45 (BC)	HI30	Biolegend
156Gd	ILT2	GHI/75	Fluidigm	198Pt	KIR2DL2/L3/S2/S4	180704	R&D Systems
158Gd	ILT2/LIR6	586326	R&D Systems	209Bi	CD16	3G8	Fluidigm
159Tb	NKp80/ NKp30	239127/ Z25	R&D Systems/ Fluidigm				
160Gd	CXCR6	K041E5	Fluidigm				

Table S6. Mass cytometry antibody panel used to characterise the Validation Cohort, related to Figures 4 and 5. CD45-specific antibodies used for barcoding are indicated with (BC) in the table.

Table S7

Study Number	Lymphocytes $\times 10^9/L$	NK cells % from total lymphocytes	Absolute Count of NK cells	Study Number	Lymphocytes $\times 10^9/L$	NK cells % from total lymphocytes	Absolute Count of NK cells
C23	2	11.984	0.239674	C38	5.5	8.6934	0.478137
C24	1.9	9.1177	0.173236	C39	2	3.6367	0.072734
C25	3.5	7.2734	0.254569	C40	0.9	8.4769	0.076292
C26	N/A	2.944	N/A	C41	3	6.3382	0.190146
C27	2.2	11.118	0.244592	C42	1.5	6.3902	0.095853
C28	2.5	2.0261	0.050653	C44	1.8	11.689	0.210407
C29	3.3	6.9097	0.22802	C45	0.8	7.9574	0.063659
C30	2	6.6499	0.132998	C46	3.5	3.6194	0.126679
C31	2	5.6369	0.112738	C47	6	1.5759	0.094554
C32	2.8	1.1862	0.033214	C48	1.5	24.652 (high)	0.369773
C33	1.2	5.5849	0.067019	C49	1.3	5.6801	0.073841
C34	2.2	3.5674	0.078483	C50	1.9	4.39	0.08341
C35	0.9	2.563	0.023067	C51	1.6	2.8574	0.045718
C36	6.2	9.3255	0.578181	C52	2.6	5.5676	0.144758
C37	4.5	5.0394	0.226773	C53	2.1	7.7496	0.162742
				C54	3.3	6.9703	0.23002

Table S7. Lymphocyte count, NK cell frequency and absolute count of NK cells for patients C23-C54 (validation cohort), related to Figures 4 and 5. Values below the normal range for each child are shown in red font. Note that the normal range for lymphocytes and NK cells in children varies with age. The normal range appropriate for each child's age has been used to determine which values are abnormal.

Figure S1

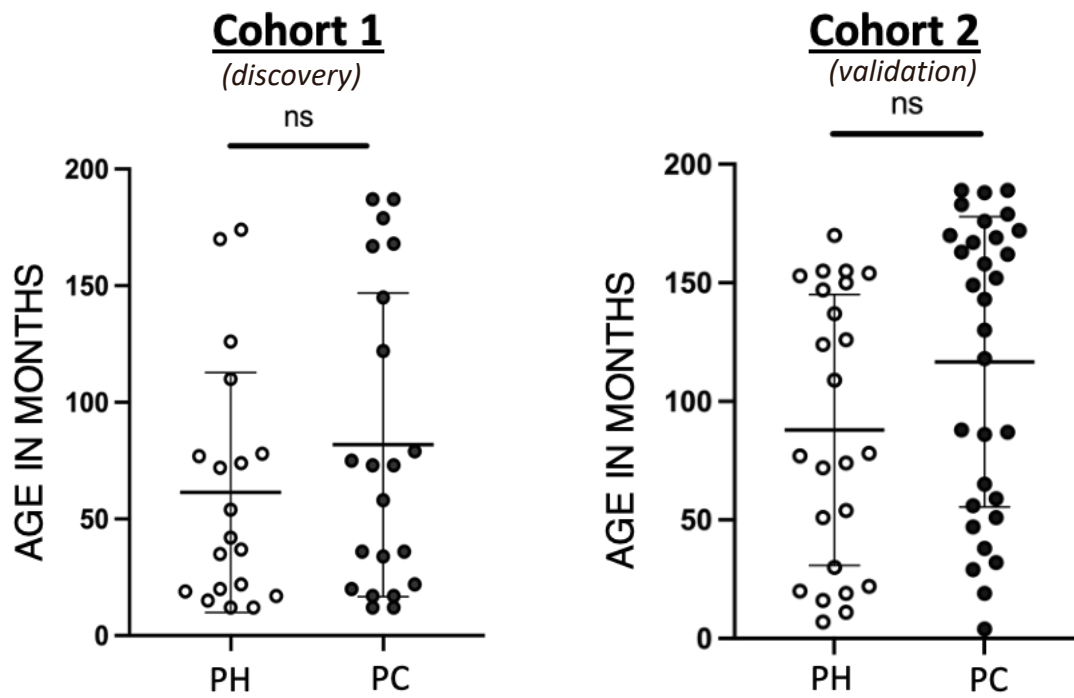


Figure S1. Age distribution of paediatric healthy (PH) or paediatric cancer (PC) donors, related to Figures 1-6. Error bars show mean \pm 1 standard deviation. There was no significant difference in age between the two groups (unpaired t-test).

Figure S2

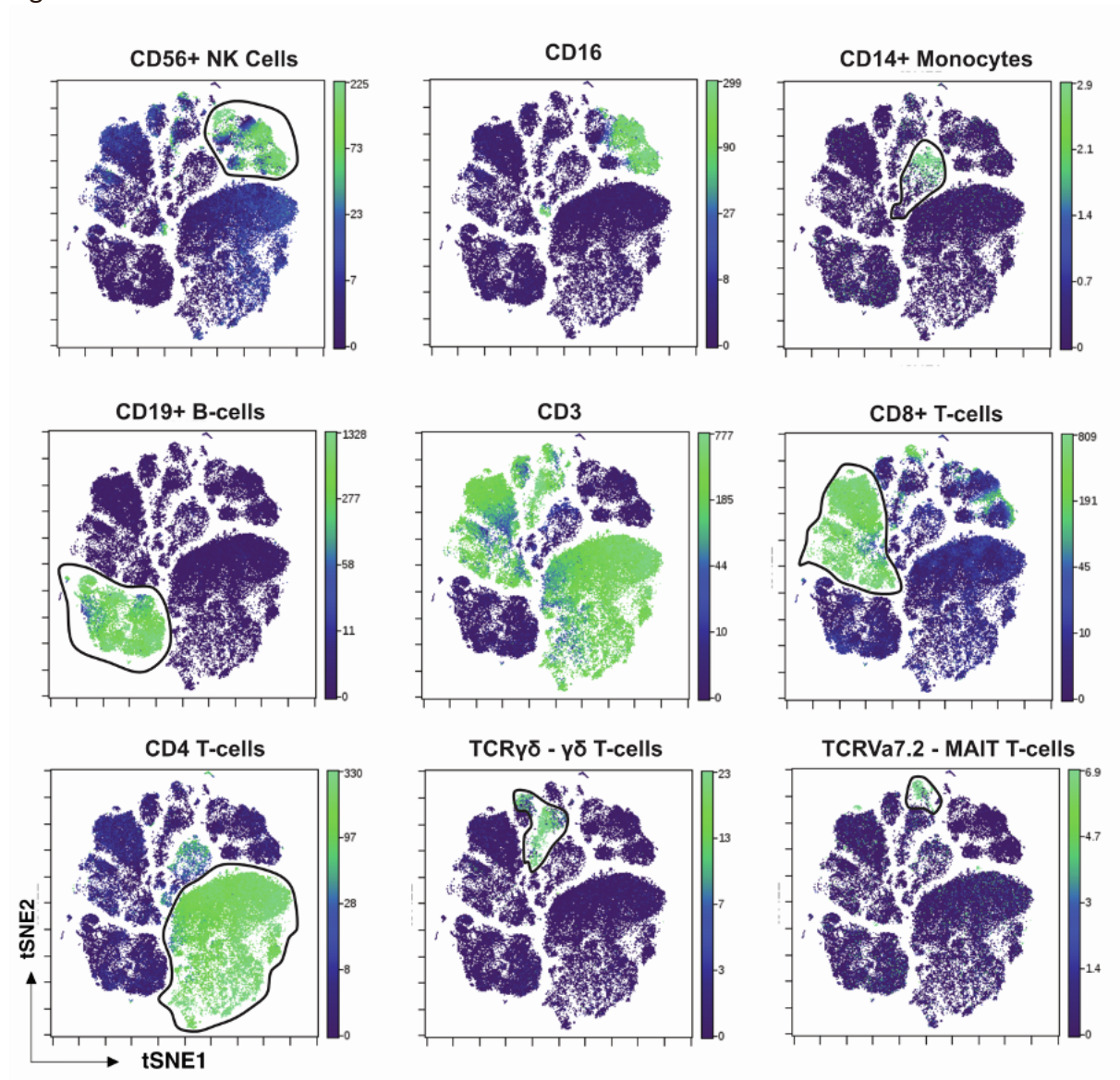


Figure S2. Gating strategy used to separate total immune cells into subsets for further analysis for discovery cohort, related to Figures 1 and 2. Each subset is determined by the indicated marker. Intensity of staining is represented by colour, with levels shown on the right-hand side of each plot.

Figure S3.

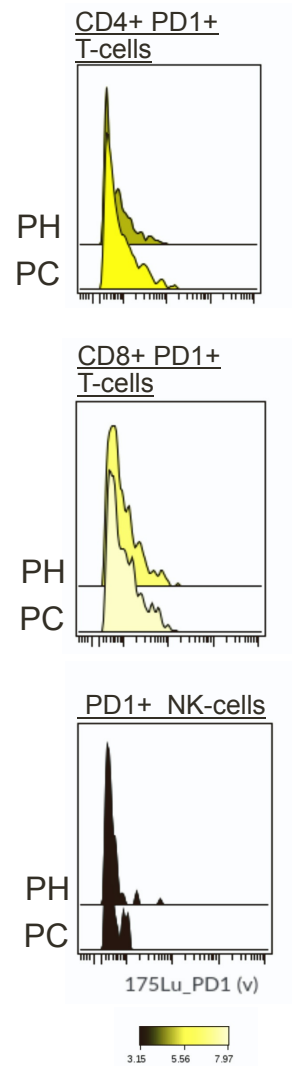


Figure S3. Median metal intensity (MMI) of PD1 on T-cells and NK cells, related to Figure 2. Levels of cell surface PD1 for the pediatric healthy and pediatric cancer patients for the discovery cohort are shown. For the total cohort the PD1 MMIs for the PD1-positive cells were: CD4 T-cells, mean 5.5, median 5.1 (range 3.8-11.8); CD8 T-cells, mean 8.4, median 7.8 (range 5.5-14.9); NK-cells, mean 3.1, median 3.0 (range 2.5-4.3).

Figure S4

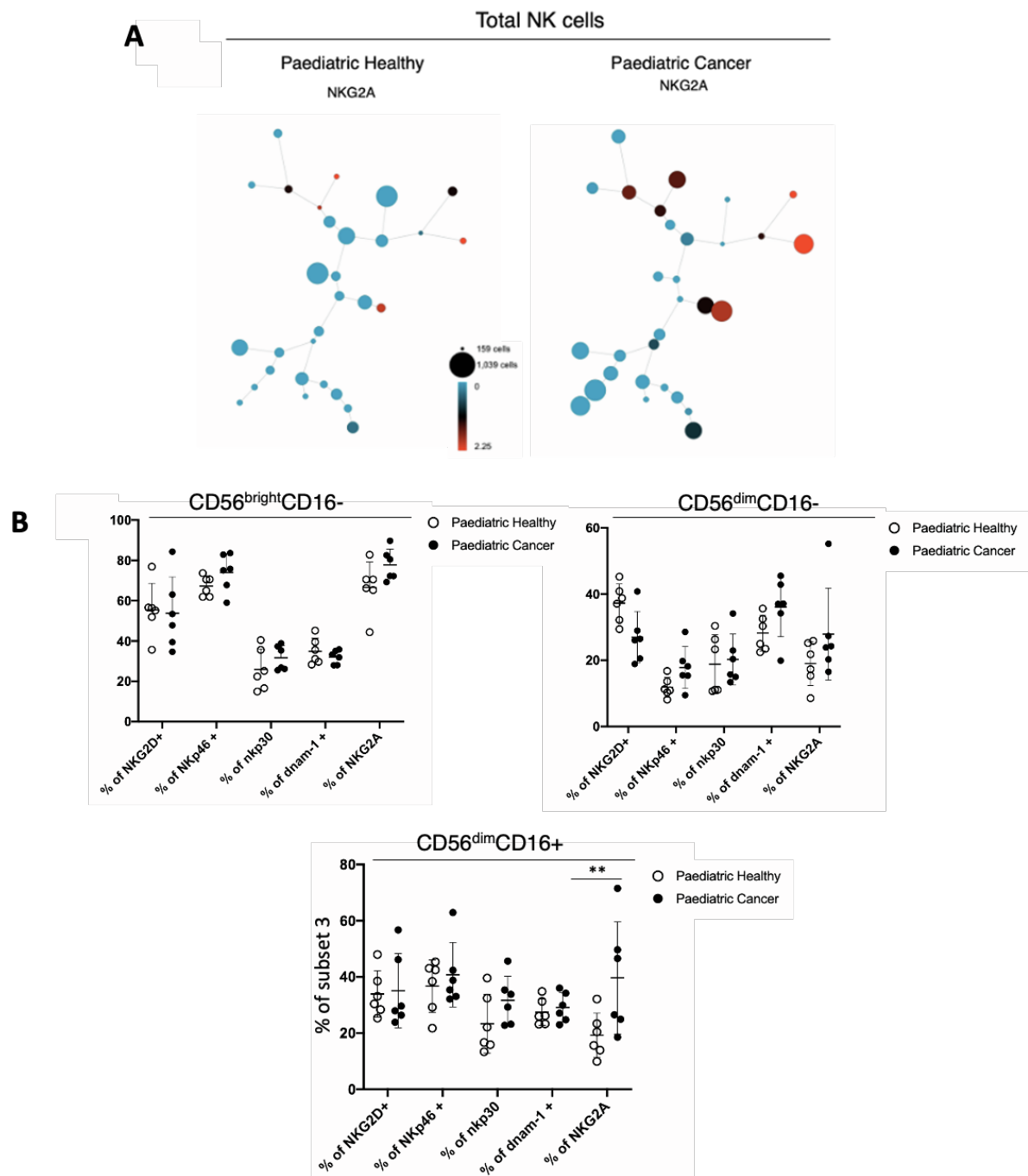


Figure S4. Analysis of NK cell receptors, related to Figure 3. A) Total NK cells were clustered using the SPADE algorithm in Cytobank. Spade nodes are coloured by the level of NKG2A expression. Size of each node reflects the numbers of cells. B) Frequency of NK cells within each of four NK cell subsets (defined using CD16 and CD56) showing the percentage of cells positive for each NK receptor. The error bars show the mean +/- one SD. Unpaired t-tests, correcting for multiple comparisons with 5% FDR, were performed with significant results indicated by an asterisk: * $p < 0.05$, ** $p < 0.01$, *** $p < 0.001$.

Figure S5

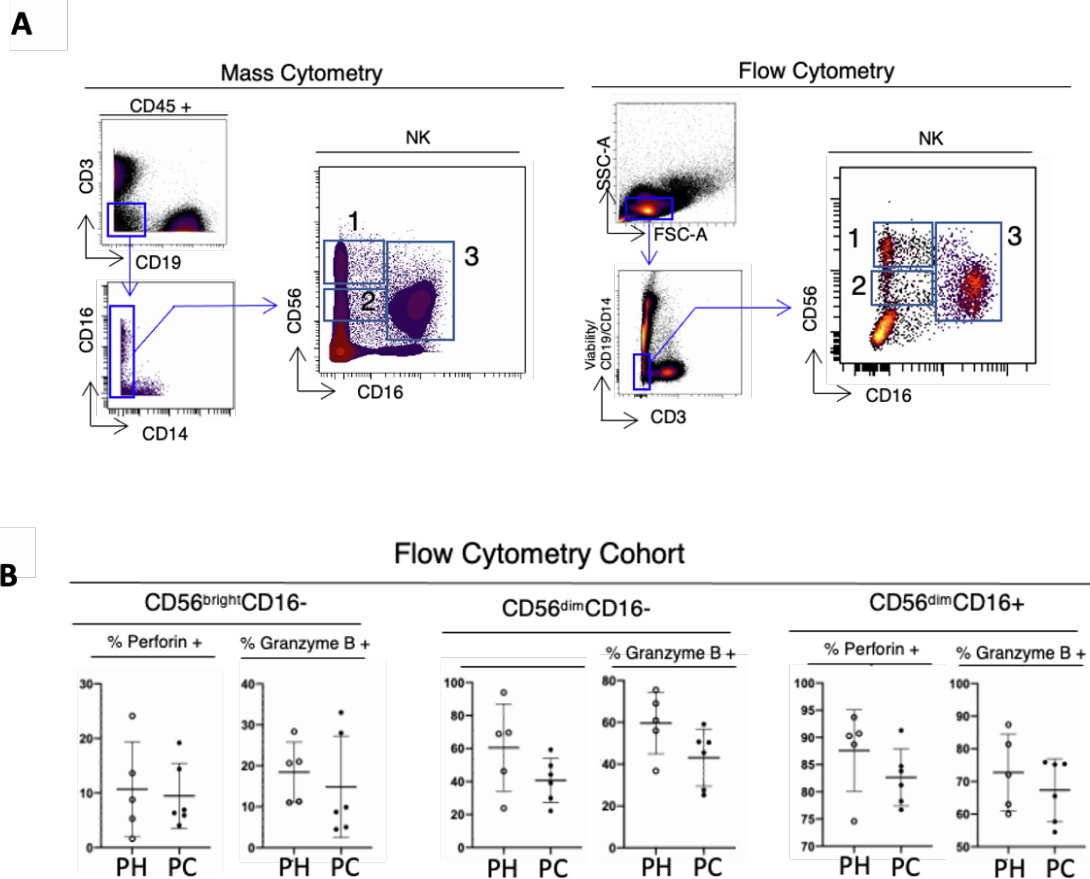


Figure S5. Perforin and granzyme B expression in NK cells, related to Figure 3. A) Gating strategy used to investigate the three NK cell subsets (defined using CD16 and CD56) from mass and flow cytometry data. B) Frequency of NK cells within each NK subset showing the percentage of cells positive for perforin or Granzyme B. The error bars show the mean +/- one SD. Unpaired t-test, correcting for multiple comparisons with 5% FDR, were performed with no significant results identified.

Figure S6

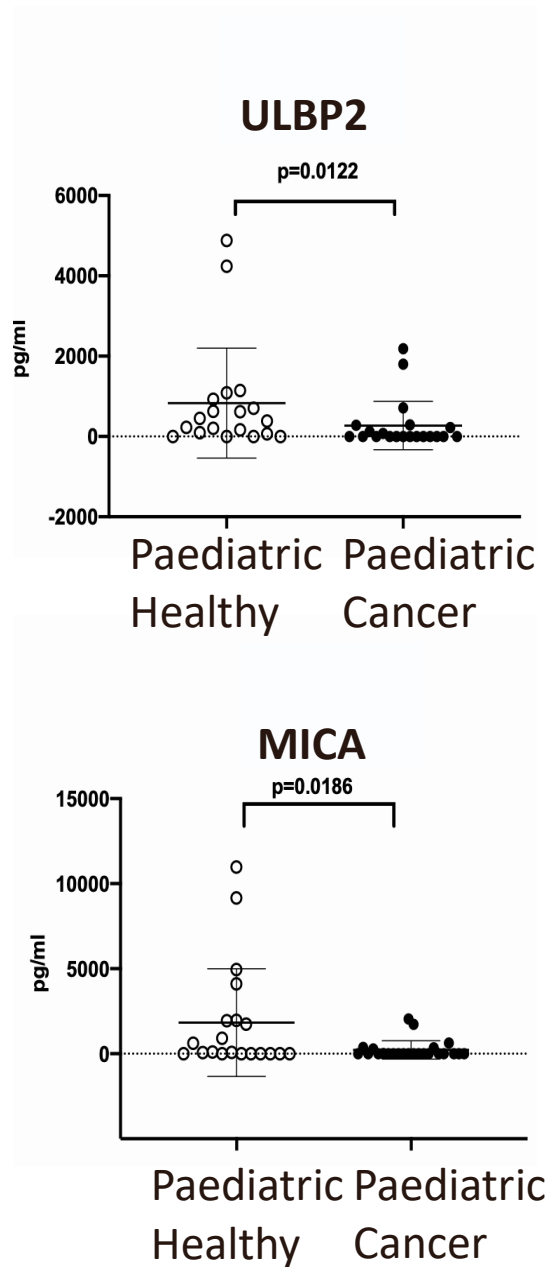


Figure S6. Results of ELISAs measuring NKG2D ligands ULBP2 or MICA in plasma, related to Figure 3. The error bars show the mean +/- one SD. Mann-Whitney tests were used to compare paediatric healthy and paediatric cancer patients (ULBP-2, $p=0.0122$; MICA, $p=0.0186$).

Figure S7

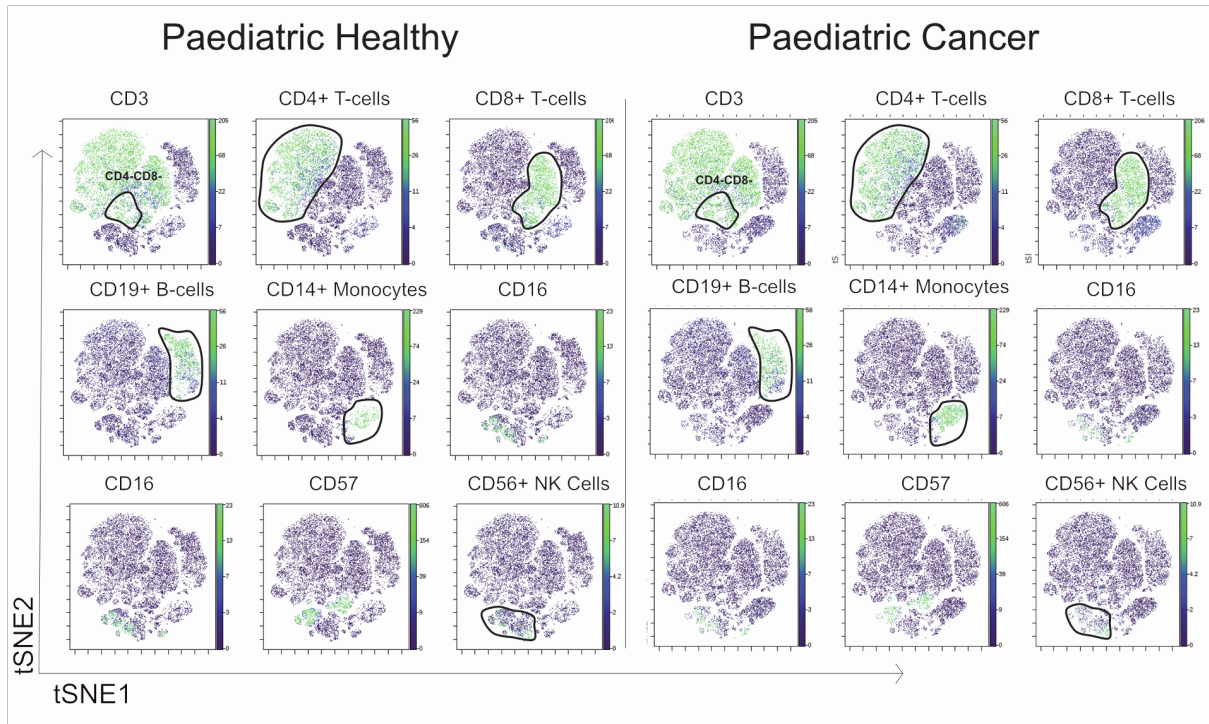


Figure S7. Gating strategy used to separate total immune cells into subsets for further analysis, related to Figure 4. Each subset is determined by the indicated marker. Intensity of staining is represented by colour, with levels shown on the right-hand side of each plot.

Figure S8

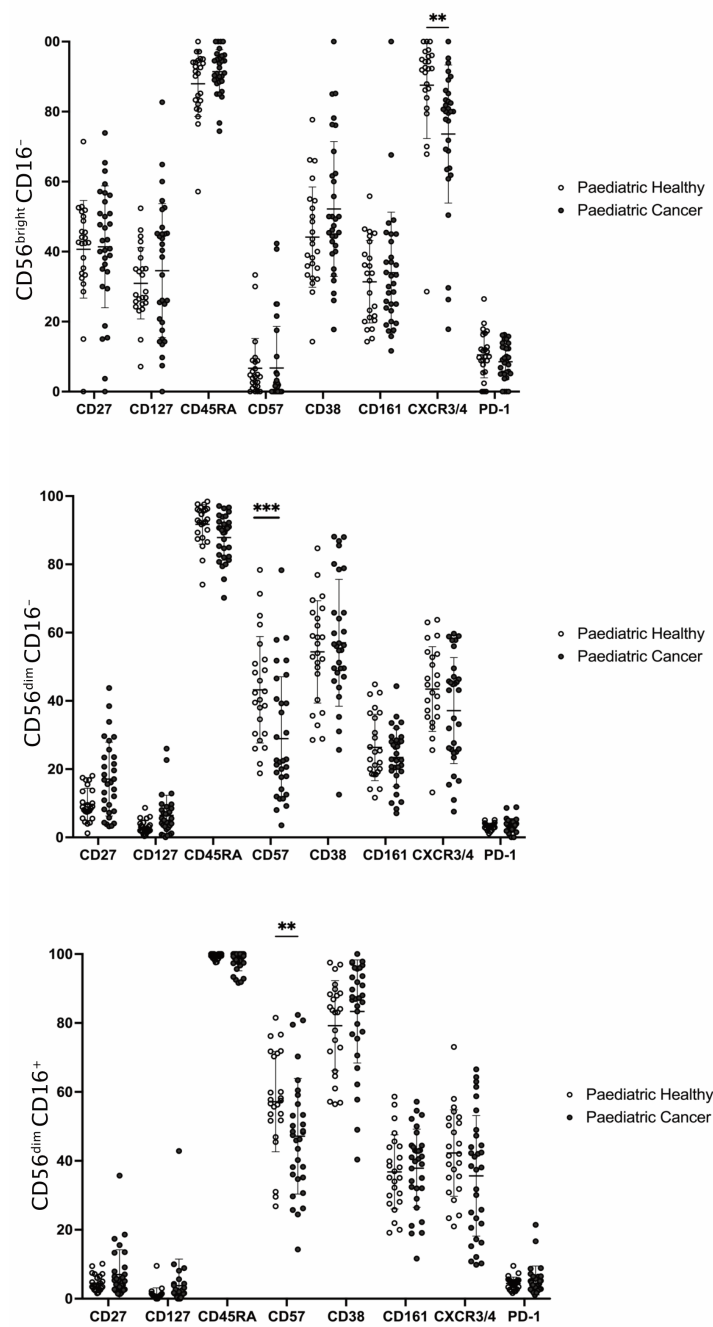


Figure S8. Percentage of cells within each NK cell subset positive for cell surface molecules, related to Figure 4. The error bars show the mean \pm one standard deviation. P values were calculated using Wilcoxon ranked sum tests with false discovery rate at 5% and correction using the Benjamini-Hochberg method. Significant results are indicated: * $p < 0.05$, ** $p < 0.01$, *** $p < 0.001$.

Figure S9

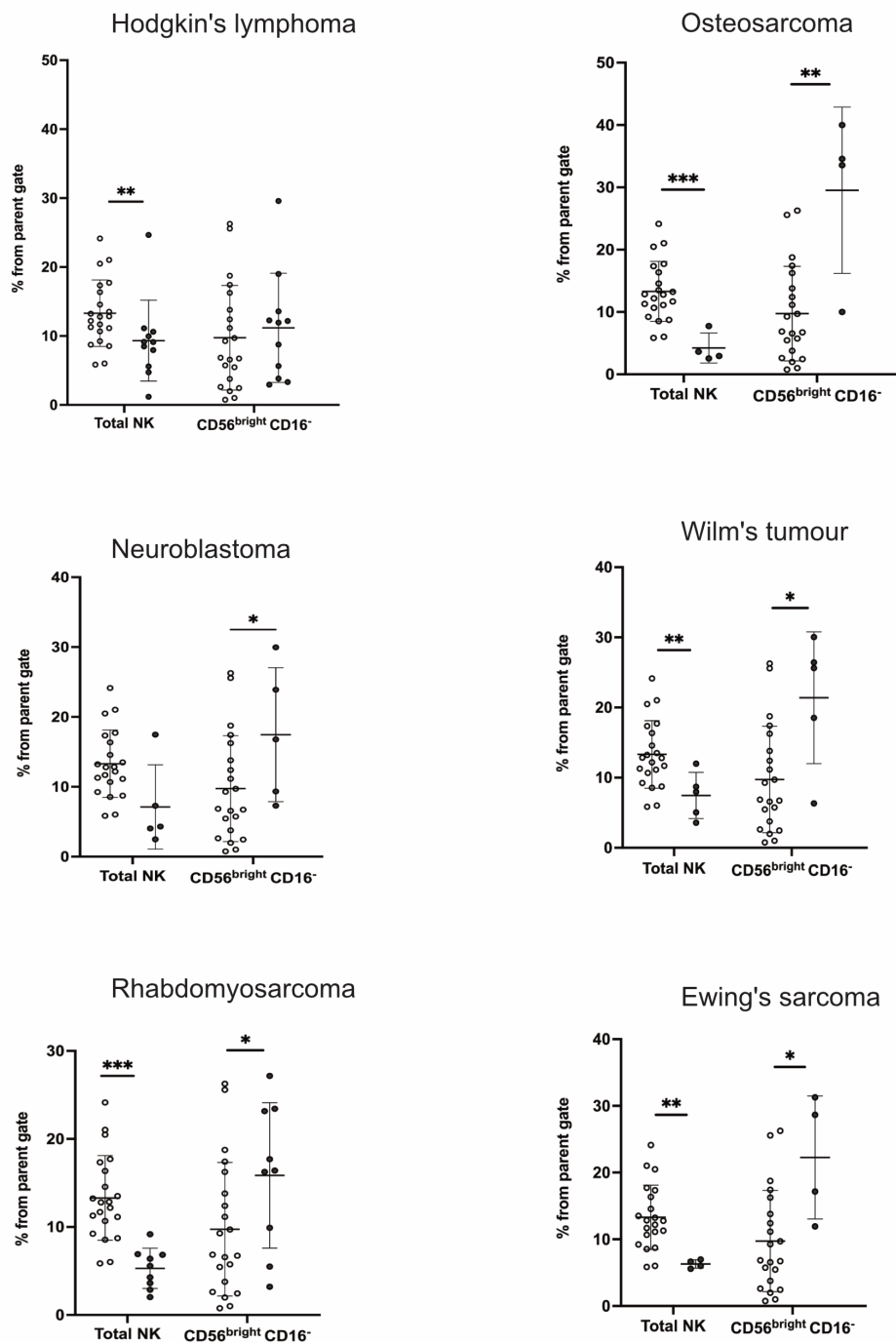


Figure S9. NK cell frequencies in patients with different cancer types, related to Figures 4 and 5. Total NK cell and CD56^{bright}CD16⁻ NK cells were analysed for each individual for the six most common paediatric cancers as shown. The error bars show the mean +/- one standard deviation. P values were calculated using Wilcoxon ranked sum tests with false discovery rate set at 5% and correction using the Benjamini-Hochberg method. Significant results are indicated as: * p<0.05, ** p<0.01, *** p<0.001

Figure S10

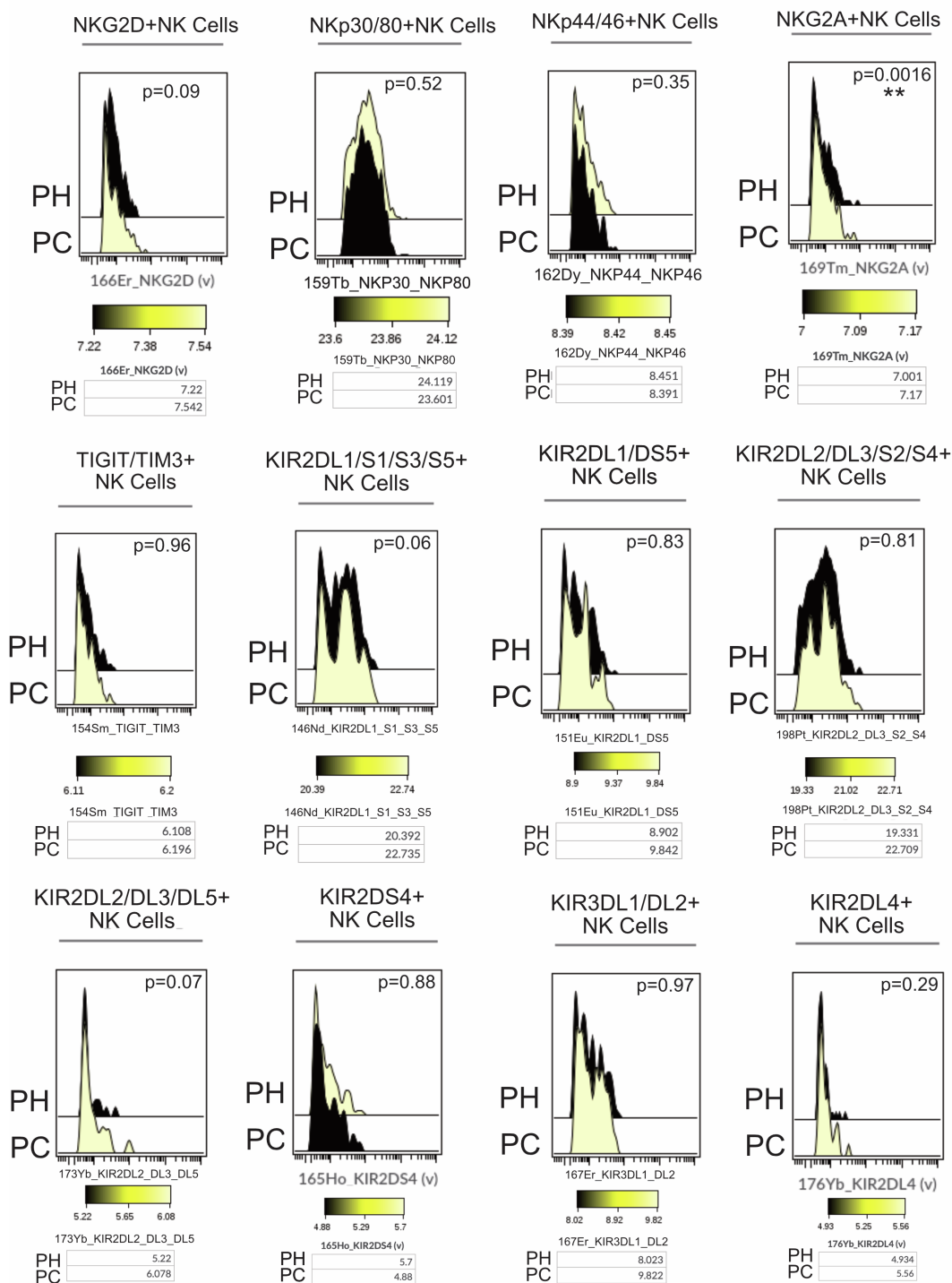


Figure S10. Median metal intensity (MMI) of NK cell receptors, related to Figure 5. The median metal intensity of each marker on NK cells gated within the positive gate for that marker are shown. P values were calculated using Wilcoxon ranked sum tests with false discovery rate at 5% and correction using the Benjamini-Hochberg method. Significant results are indicated: * $p < 0.05$, ** $p < 0.01$, *** $p < 0.001$.

Figure S11

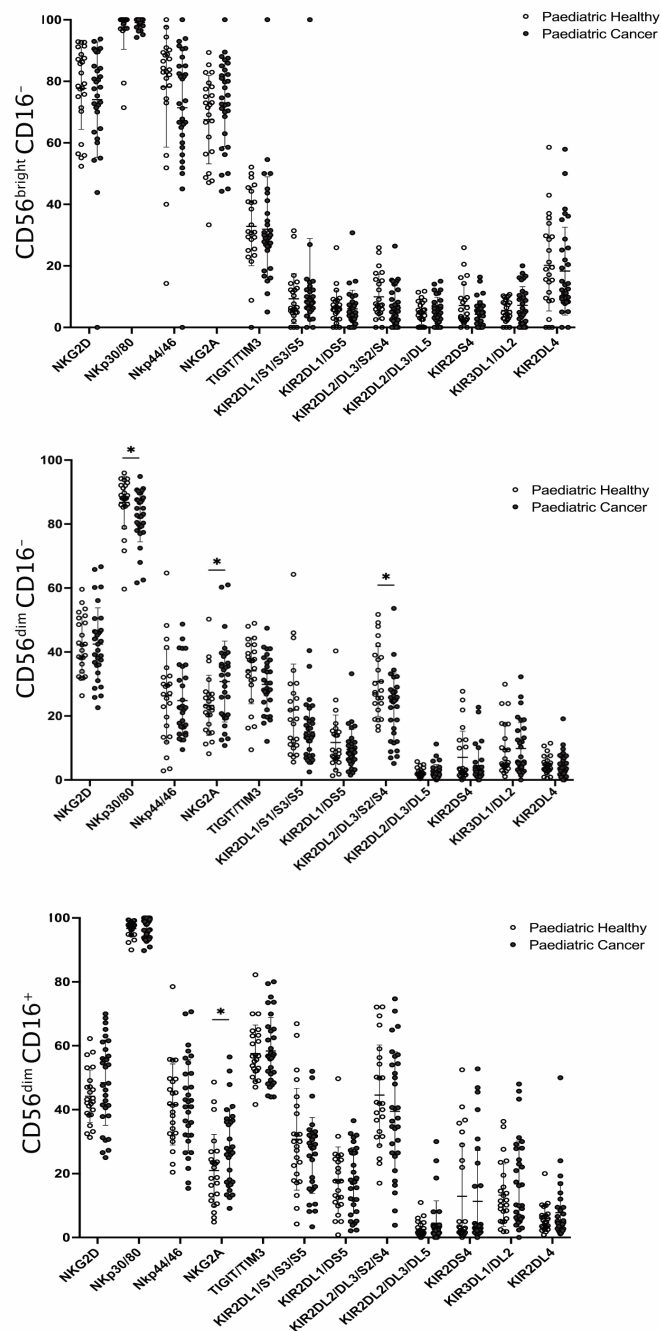


Figure S11. NK cell receptor expression for each NK subset. Values are shown for each individual, related to Figure 5. The error bars show the mean +/- one standard variation. P values were calculated using Wilcoxon ranked sum tests and are shown in the figure. When we applied a false discovery rate set at 5% and used the Benjamini-Hochberg multiple comparison correction method no statistical significant results were identified. Significant results indicated as: * p < 0.05, ** p < 0.01, *** p < 0.001 are before multiple comparison correction.